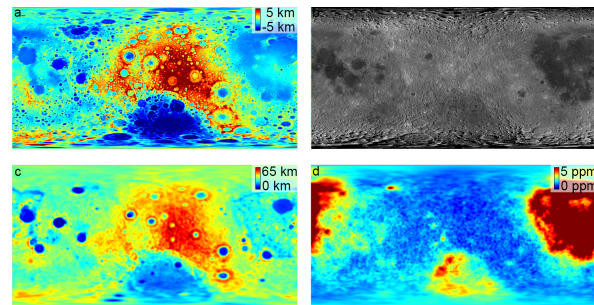


**FORMING THE LUNAR ASYMMETRIES.** J. C. Andrews-Hanna<sup>1</sup>, A. J. Evans<sup>2</sup>, and A. Mallik<sup>1</sup>, <sup>1</sup>Lunar and Planetary Laboratory, University of Arizona, Tucson, AZ ([jcahanna@arizona.edu](mailto:jcahanna@arizona.edu)), <sup>2</sup>Department of Earth, Environmental and Planetary Sciences, Brown University, Providence, RI.

**Introduction:** The Earth's Moon is fundamentally asymmetric – in topography, crustal thickness, geochemistry, and volcanic history. The lunar topographic asymmetry is expressed as a strong spherical harmonic degree-1 component to the shape (a cosine function from one hemisphere to the other) with a total amplitude of 3.9 km [1]. Similarly, the crustal thickness asymmetry is expressed as a spherical harmonic degree-1 pattern with a total amplitude of 17 km [2]. The isostatic compensation of the crust explains the topographic asymmetry. Within the thin crust of the nearside, an enrichment in potassium, rare earth elements, phosphorus (KREEP) and other incompatible elements defines the Procellarum KREEP terrane (PKT) [3]. The nearside hosts the majority of the volcanic maria, likely as a result of the combined effects of the thin crust and enhancements in heat producing elements. This region also contains high concentrations of titanium, though the maria, KREEP and titanium follow somewhat different spatial distributions. The generation of the plagioclase-rich crust, as well as high concentrations of both KREEP and titanium (the latter likely in the form of dense ilmenite bearing cumulates, or IBCs), are a natural outcome of the end stages of magma ocean crystallization [4]. However, the cause for the asymmetric distribution of the crust, KREEP, and IBCs remains a major outstanding question.

The degree-1 nature of the crustal asymmetry favors simple mechanisms that fundamentally predict a degree-1 pattern. The crust was generated from the crystallization of a magma ocean, and we here show that magma ocean processes can, under some conditions, naturally lead to the observed asymmetry.

**Crustal asymmetry as a consequence of magma ocean crystallization:** The development of a global asymmetry is a natural outcome of any scenario in which a layer of material exists with a higher density than the bulk density of the underlying lunar interior. Such a scenario is buoyantly unstable. If the over-dense layer has a sufficiently lower viscosity than the underlying material, then a lower potential energy state can be achieved in which the over-dense material “sloshes” to one hemisphere, offsetting the solid interior toward the opposite hemisphere. Conceptually, this can be easily understood in terms of the tendency of the under-dense interior to float upward toward the surface through the over-dense overlying material, with “upward” being any direction in an initially spherically symmetric geometry. The dense material then forms a



**Figure 1.** Global maps showing the **a** topographic, **b** crustal, **c** volcanic, and **d** compositional (Th abundance) asymmetries (centered on the farside).

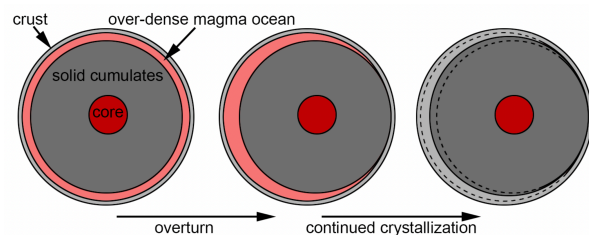


**Figure 2.** Degree-1 instability of an over-dense magma ocean layer, followed by continued crust formation.

lens in one hemisphere. The resulting asymmetry is the lowest potential energy state achievable, until the dense material finds its way to the center of the body. This mechanism was previously explored in the context of an asymmetric iron core above a cold solid interior [5], and for the solid state creep of a dense layer of IBCs after magma ocean crystallization to explain the PKT [6].

If a density inversion and degree-1 instability developed during magma ocean crystallization while the crust was still forming, it could explain the observed crustal asymmetry. The densities of the residual magma ocean and the forming cumulates increase during magma ocean crystallization as iron and other dense oxides become progressively concentrated in the residual liquid [7, 8]. If the density of the remaining magma ocean exceeds the bulk density of the underlying solid interior ( $\sim 3400 \text{ kg/m}^3$ , after removing the low-density crust), a degree-1 instability will develop and the magma ocean will rapidly migrate toward one hemisphere (here assumed to be the farside), while the underlying solid interior rises to the other hemisphere. This instability will result in a degree-1 variation in the depth of the magma ocean. Continued crystallization will preferentially thicken the crust above the thicker magma ocean in the farside hemisphere, while the crust in the central nearside

maintains constant thickness, generating a degree-1 variation in crustal thickness.

The degree-1 variation in crustal thickness of ~17 km relative to a mean thickness of ~34 km would be brought about if the density inversion and magma ocean migration occurred when crust formation was 75% complete, or at 95 percent solidification (PCS) of the magma ocean, assuming plagioclase floatation begins at 80 PCS. At this point, the Moon would have possessed a uniform crust ~26 km thick. After the instability, continued crustal thickening would follow a degree-1 pattern, leading to a crustal thickness of 43 km on the farside and 26 km on the nearside.

The question then becomes whether this density inversion can be brought about. The required inversion at 95 PCS corresponds with predicted increases in magma and cumulate density in a number of studies [e.g., 4, 7, 8]. Some thermodynamic models predict the magma ocean itself to become more dense than the solid interior as early as 81-83 PCS, shortly after plagioclase begins to crystallize [4, 8]. In contrast, laboratory experiments indicate that the magma ocean density increases to ~3000-3100 kg/m<sup>3</sup> at ~95 PCS, but remains lower than the solid interior density [7]. However, at the same time, the forming cumulates become increasingly dense. After floatation of the buoyant plagioclase, the remaining cumulates attain average densities of ~3500-3900 kg/m<sup>3</sup> at ~95 PCS [7]. For a convecting magma ocean, a substantial fraction of these cumulates may remain entrained in the magma, increasing the bulk density of the magma-crystal mixture. For magma and crystal densities of 3100 and 3900 kg/m<sup>3</sup>, the mixture would exceed the density of the solid interior for a crystal fraction of >38%. A viscosity more similar to the liquid than the solid is expected for crystal fractions up to 50% [9], resulting in large viscosity contrasts enabling the overturn [6]. After the magma ocean instability, the magma ocean depth would double on the farside, increasing the radiogenic heat flux and remelting the crystal mush to enable continued formation of the floatation crust

**Forming the compositional asymmetry:** Once the crustal asymmetry is created, it is then necessary to explain the compositional asymmetry. However, forming the crustal and compositional asymmetries requires a dramatic reversal – the late stage KREEP- and Ti-rich materials that crystallize during crustal formation should have preferentially formed where the crust and magma ocean were thickest, yet they must become concentrated where the crust is thinnest. The IBCs form during the final 5-10% of MO crystallization, and, for the scenario described above, would have formed a dense lens between the mantle and crust on the farside, sitting in a gravitational potential energy well.

Subsequent migration of the IBCs to the nearside would increase the potential energy of the system, effectively requiring the over-dense cumulates to move “uphill”. However, the concentration of heat producing elements in the late stage magma ocean products in one hemisphere (in this case, the farside where the crust is thickest) would result in the gradual warming and uplift of that hemisphere [10, 11]. The resulting uplift of ~10 km over several 100 Myr could have raised the dense IBCs such that their migration to the nearside was no longer resisted by gravity. Migration to the nearside may then have occurred through a second degree-1 instability toward the opposite hemisphere [6] or may have been facilitated by the mantle flow patterns in response to the South Pole-Aitken impact [12, 13].

KREEP-rich material would have concentrated in the final liquids. The KREEP-rich materials may have migrated toward the nearside together with the IBCs. Alternatively, separation of the KREEP-rich liquids from the dense cumulates may result in a buoyant melt. These liquids would naturally concentrate where the crust is thinnest beneath nearside. By 99.8 PCS (1 km global equivalent layer) the final liquids of the magma ocean would be concentrated exclusively beneath the thin crust of the present-day PKT.

**Conclusions:** The lunar crustal asymmetry could be brought about by an increase in magma ocean density to >3400 kg/m<sup>3</sup> at ~95 PCS, either from a direct increase in magma density or entrainment of dense cumulates. While such a density inversion cannot be ruled out, it may be difficult. However, there are many uncertainties regarding the details of magma ocean crystallization, including starting composition, water content, relative importance of fractional and equilibrium crystallization, and the efficiency with which crystals are extracted from the melt. Given that the Moon does exhibit a prominent crustal thickness asymmetry which has yet to be conclusively explained, and that this asymmetry can be explained by a density inversion in the magma ocean, mechanisms for bringing this about are worth exploring.

**References:** [1] Smith, D.E. et al., (2010), *GRL* **37**, L18204. [2] Wieczorek, M.A. et al., (2013), *Science*, **339**, doi:10.1126/science.1231530. [3] Wieczorek, M.A., Phillips, R.J., (2000), *JGR* **105**, 20,417-20,430 [4] Elkins-Tanton, L.T. et al., (2011), *EPSL* **304**, 326–336. [5] Stevenson, D.J., (1980), *Nature*, **287**, 520–521. [6] Parmentier, E.M. et al., (2002), *EPSL* **201**, 473–480. [7] Schmidt, M.W., Kraettli, G., (2022), *JGR* (2022), doi:10.1029/2022JE007187. [8] Elkins-Tanton, L.T., Bercovici, D., (2014), *Philos. Trans. R. Soc. A* **372**, doi:10.1098/rsta.2013.0240. [9] Arai, T., Maruyama, S., (2017), *Geosci. Front.* **8**, 299–308. [10] Laneuville, M. et al., (2013), *JGR* **118**, 1435–1452. [11] Grimm, R.E., (2013), *JGR* **118**, 768–778. [12] Jones, M.J. et al., (2022), *Sci. Adv.* **8**, eabm8475, doi:10.1126/sciadv.abm8475. [13] Zhang, N. et al., (2022), *Nat. Geosci.* **15**, 37–41.